The Structure of Ferritin Cores Determined by Electron Nanodiffraction

J. M. Cowley,*,[1] Dawn E. Janney,†,‡ R. C. Gerkin,*,[2] and Peter R. Buseck†,‡

*Department of Physics and Astronomy, †Department of Geology, and ‡Department of Chemistry/Biochemistry, Arizona State University, Tempe, Arizona 85287

Electron nanodiffraction, with a 100-keV electron beam less than 1 nm in diameter, has been used to obtain single-crystal diffraction patterns from individual iron-containing cores of ferritin molecules. We show that, while a majority of the cores have a hexagonal structure somewhat similar to the major phase in the mineral ferrihydrite, as previously assumed, several minor phases are present including some that are similar in structure to the iron oxides magnetite and hematite and also some composed of highly disordered material. In general, each core consists of one single crystal of one phase. © 2000 **Academic Press**

Key Words: **electron nanodiffraction; ferrihydrite; ferritin cores; iron oxides; scanning transmission electron microscopy; structural disorder.**

INTRODUCTION

It has been known for many years that the protein shell of the ferritin molecule encloses an iron-rich core. For ferritin from mammals and some other organisms, this core appears to be crystalline with a structure similar to that of the mineral ferrihydrite. Comprehensive reviews of the state of knowledge on the structure of the molecule and its core have been given, for example, by St. Pierre *et al.* (1989), Massover (1993), and Chasteen and Harrison (1999).

The outer shell of the ferritin molecule has been shown by X-ray diffraction analysis to consist of 24 protein subunits of two kinds. The outer diameter of the shell is 13 nm, and the iron-containing core forms within an inner, roughly spherical space of 8 nm in diameter. The core may fill, or partially fill, the inner space. The evidence from electron microscopy (Massover, 1993) suggests that the core may consist of a single crystal or of several small crystals, apparently nucleated at different points within the protein shell.

Ferrihydrite is a common iron oxide–hydroxide mineral formed in low-temperature environments. It is important in environmental science and in industry where it is commonly known as "amorphous" or "colloidal" ferric hydroxide (Jambor and Dutrizac, 1998). Because the crystallite size is 6 nm or less, the X-ray and selected-area electron diffraction (SAED) patterns show just a few diffuse lines (Towe and Bradley, 1967; St. Pierre *et al.,* 1989; Janney *et al.,* 2000a). The so-called six-line ferrihydrite (6LFh) preparations show six diffuse diffraction peaks corresponding to *d*-spacings of 0.15 (a doublet), 0.17, 0.20, 0.22, and 0.25 nm. Other preparations, designated 2LFh, showing only two very diffuse diffraction lines at 0.15 and 0.25 nm, have been thought of as being much the same as 6LFh but having a less crystalline form (Drits *et al.,* 1993b).

The structure of the ferritin core material is not well established. Identification with the structure of six-line ferrihydrite comes from the similarity of X-ray powder diffraction and selected-area electron diffraction patterns (Harrison *et al.,* 1967; Towe and Bradley, 1967; St. Pierre *et al.,* 1989) and from the periodicities of fringe patterns observed in high-resolution electron microscopy images (Massover and Cowley, 1973; Massover, 1993).

Recently, we studied the structures of several ferrihydrite samples and ferritin cores using electron nanodiffraction. In this technique, diffraction patterns are obtained with a 100-keV electron beam focused to a diameter of less than 1 nm so that single-crystal patterns can be obtained from regions within individual crystallites a few nanometers in diameter. It has been shown in this way that the accepted notions concerning the structures of these materials must be revised. The 2LFh and 6LFh ma-
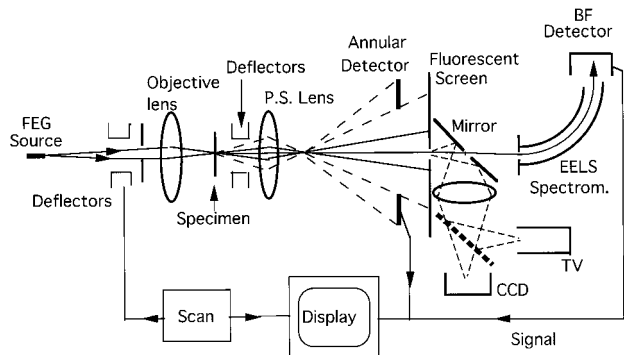
FIG. 1. Diagram of a STEM instrument. The intense electron beam from a field-emission gun (FEG) is focused on the specimen by the objective lens. The convergent beam electron diffraction pattern is formed on the fluorescent screen after being magnified by a postspecimen (PS) lens and is observed and recorded by use of a TV–VCR system or a CCD camera. STEM images are formed by scanning the beam over the specimen and displaying the signal formed by an annular detector in the diffraction plane or by passing part of the diffraction pattern through an aperture and an electron-energy-loss spectrometer (EELS).

terials have basically different structures and are, in each case, not single phases but mixtures of related phases (Janney *et al.,* 2000c, 2000b). The ferritin cores and the 6LFh samples are similar in that they have one major phase in common, but in each case there are several minor phases present and these minor phases differ in their nature and/or their relative proportions. The analysis of the structures occurring in the 6LFh samples is reported elsewhere (Janney *et al.,* 2000c). In the present paper we report the results of the nanodiffraction studies of ferritin cores.

METHODS

The specimens of ferritin were prepared from standard commercial horse-spleen ferritin (Sigma Chemical Co., St. Louis, MO). Synthetic ferrihydrite is commonly synthesized at about 75°C (Janney *et al.,* in press); the most common method of purification of ferritin involves heating a tissue homogenate to about this same temperature. Samples of ferritin were dispersed on a thin carbon film so that the individual molecules were well separated, with no overlapping.

The ferritin specimens were examined with electron beams of 100 keV in energy in an HB-5 scanning transmission electron microscopy (STEM) instrument from VG Microscopes, Ltd., specially modified to allow the convenient observation and recording of nanodiffraction patterns and bright- or dark-field images with various detector configurations (Cowley, 1995, 1999) (see Fig. 1).

In nanodiffraction, the electron beam is focused on the specimen to form a cross-over of diameter as small as 0.3 nm, roughly equal to the resolution attainable for dark-field STEM images. The convergent-beam diffraction pattern formed on a fluorescent screen is viewed by means of a low-light-level television camera and recorded by a videocassette recorder (VCR) or else is recorded digitally by the use of a CCD camera. With the TV–VCR arrangement, diffraction patterns may be recorded at a rate of 30 per second. A series of diffraction patterns may be recorded as the

incident beam is scanned slowly over the specimen. Alternatively, an electronic marker is used to identify the point in the image of the specimen from which the diffraction pattern is obtained when the beam is stopped. With the CCD recording system, the very weak diffraction patterns from regions containing only a few hundred atoms may be recorded with an exposure time of about 1 s.

For the observation of nanodiffraction patterns from ferritin cores, a small aperture in the objective lens limits the beam convergence angle to 3×10^{-3} rad so that the diameter of the beam focused on the specimen is about 0.7 nm. The diffraction spots are then small enough so that they are well separated for lattice plane spacings of 0.3 to 0.4 nm, but there is considerable overlapping of spots for spacings of 0.7 nm.

Patterns with sharper spots can be obtained from very small isolated crystallites such as ferritin cores by defocusing the beam as suggested in Fig. 2. For a defocus of a few micrometers, the width of the beam at the specimen may be 3–5 nm. If the crystallite diameter is less than this, the angular width of the diffraction spots is determined by the angle subtended by the crystallite at the cross-over position, and this is less than the beam-convergence angle, which determines the spot size for the in-focus patterns. The resulting patterns, such as those of Fig. 4, can now show a clear separation of diffraction spots for lattice spacings of 1 nm or more.

A disadvantage of this defocus method is that a diffraction pattern may contain spots from neighboring crystals and also a diffuse background from an amorphous carbon supporting film or, in the case of ferritin, from the protein material surrounding the
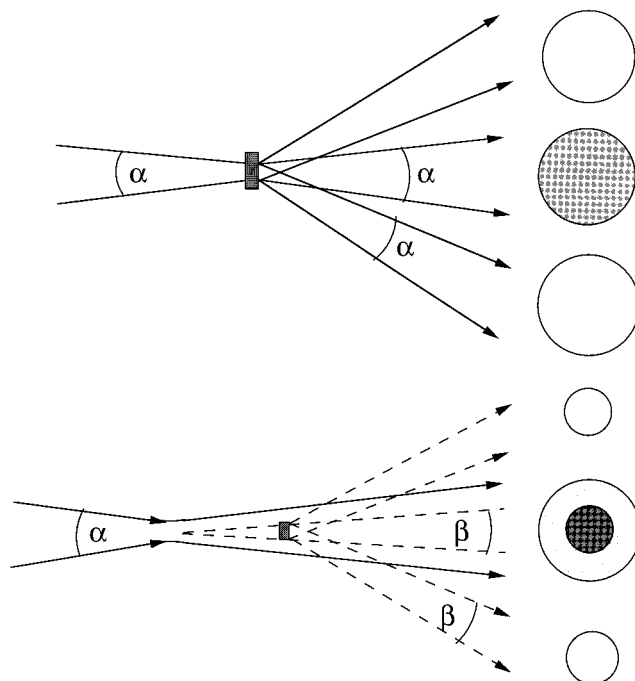

FIG. 2. The effect of defocus on the angular dimensions of diffraction spots in nanodiffraction patterns. In (a) the beam is focused on a thin specimen and the angular spread of the diffraction spots is α, the incident beam-convergence angle. In (b) the objective lens is defocused so that the beam diameter at the specimen is greater than the crystallite diameter. The size of the diffraction spot depends on the angle β subtended by the crystallite at the beam cross-over, and this is less than α.
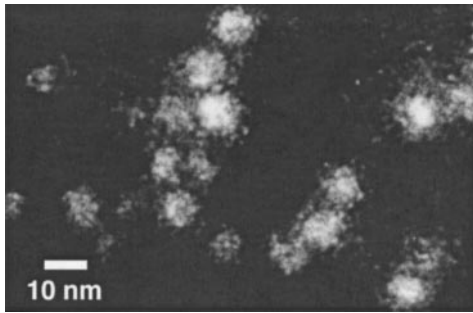
FIG. 3. Dark-field STEM image of a group of ferritin molecules obtained with a detector sensitive to diffraction intensities.

core. In the case of adjacent or partially overlapping crystallites, the contributions from the separate crystallites may sometimes be distinguished because the centers of the patterns do not coincide.

The dark-field STEM images reported in the literature have commonly been obtained by use of an annular detector that collects nearly all the electrons scattered outside the incident beam cone. The image intensities are then determined, to a good approximation, by the number and atomic number of the atoms in the part of the specimen illuminated by the incident beam (Crewe and Wall, 1970; Isaacson and Ohtsuki, 1980). Such images are not sensitive to the crystallinity of the specimen However, we have made use of a thin annular detector having inner and outer radii differing by as little as 10% (Cowley et al., 1995). With such a detector, used in conjunction with postspecimen lenses, it is possible to obtain dark-field images from regions of various ranges of radii within the diffraction pattern. These images are sensitive to the intensities of particular sets of diffraction spots and may reveal variations of crystal structure, crystal orientation, or degree of crystallinity within small particles.

RESULTS

Figure 3 is a dark-field STEM image of a group of ferritin molecules showing bright patches corresponding to the cores. This high-contrast image was obtained using a thin annular detector set to detect diffracted beams corresponding to spacings roughly in the range of 0.1 to 0.3 nm. The differences in contrast of the various core images derive mostly from differences in diffracting conditions. The core diameters average 8 nm. Apart from a mottled intensity distribution on a scale of about 1 nm, the cores show uniform contrast or else a slow variation of contrast across their images. This observation is in reasonable agreement with previous observations (Massover, 1993).

A further observation is that, if the incident beam of diameter 0.7 nm is scanned slowly across the image of one ferritin core, the diffraction pattern in most cases does not vary in form or dimension. This is a clear indication that, except in particular cases to be discussed later, the core consists of a single crystal of one phase in one orientation. No indication has been found for the occurrence of crystallites of

more than one structure or in more than one orientation within a single core.

The diffraction patterns obtained from the ferritin cores show a variety of forms as might be expected for crystallites in random orientation. Because of the small sizes of the cores and the relatively large, often erratic, displacements introduced by tilting with the available specimen holders, it is not possible to examine any single core in different orientations. However, it became clear that it was not possible to interpret the patterns in terms of different orientations of any one structure. Examination of the patterns from a large number of cores revealed sets of patterns consistent with the presence of several different crystal structures.

In particular, characteristic patterns obtained from crystallites that had almost zone-axis orientations, reproduced in Figs. 4 to 7, provided clear identification of several phases when compared with simulated patterns calculated for known and postulated iron oxide structures. Patterns were simulated for each structure in a wide range of orientations to ensure that all the patterns could not be produced by any single one of the structures identified.

The various structures found in the ferritin cores are similar to those in ferrihydrite samples, although the relative proportions of the phases are different. Table I gives rough estimates of the relative percentages of the various structures found in ferritin cores and those in two samples of 6LFh, designated 75C-6LFh and RT-6LFH, and prepared by different processes, one at 75°C and one at room temperature (Schwertmann et al., 1999; Janney et al., 2000c). The evidence for the occurrence of each of these structures is now reviewed in sequence.
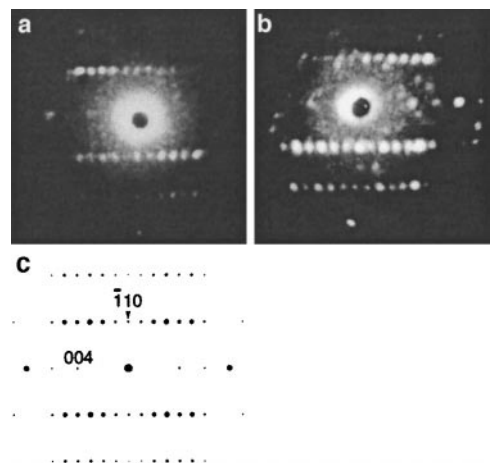

FIG. 4. Nanodiffraction patterns for the [110] orientation of the double-hexagonal structure for (a) a ferritin core and (b) a ferrihydrite crystallite (cf. Janney et al., 2000c). (c) A simulated pattern for the refined structure.
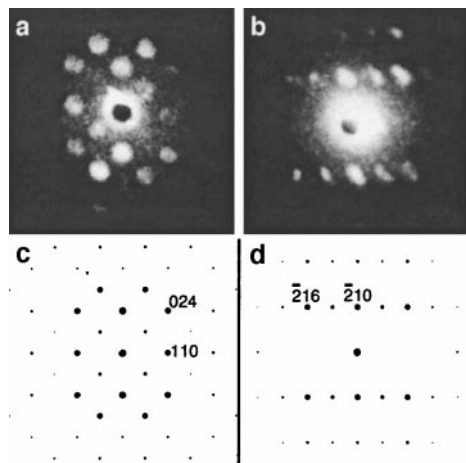
FIG. 5. Nanodiffraction patterns obtained from ferritin cores having (a) the [2,-2,1] and (b) the [120] orientations of hematite, compared with the simulated patterns, (c) and (d), for these orientations.

Double-Hexagonal Structure

It is estimated that roughly two-thirds of the ferritin cores have the same structure as the dominant phase of the six-line ferrihydrite samples. The structure is based on the distribution of iron atoms in the octahedral sites of the close-packed stacking of hexagonal layers of oxygen (or OH or possibly H_2O) in the four-layer sequence, ABAC, giving a hexagonal unit cell with dimensions $a = 0.30$ nm and $c = 0.94$ nm.

The characteristic and distinctive pattern of spots given in the [110] orientation for a ferritin core is shown in Fig. 4, compared with a similar pattern from a ferrihydrite crystallite and a simulated pattern. The intensity distributions along the closely spaced lines of spots, with separations corresponding to the 0.94-nm unit cell dimension, clearly rule out previously proposed models for this structure such as that proposed by Harrison et al. (1967) for ferritin cores and the structures proposed by Towe
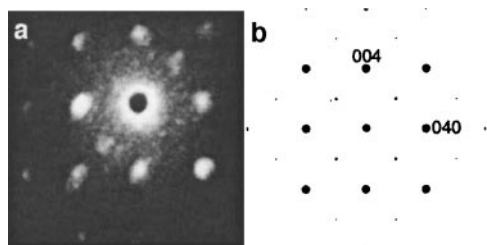

FIG. 6. Observed and simulated nanodiffraction patterns for a ferritin core having a magnetite or maghemite structure in [100] orientation.
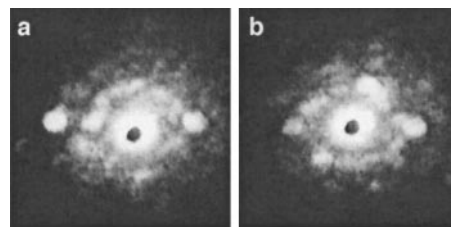

FIG. 7. Nanodiffraction patterns (a and b) obtained from adjacent regions within one ferritin core showing the diffuse streaking characteristic of a high degree of disorder.

and Bradley (1967) and by Eggleton and Fitzpatrick (1988) for ferrihydrite.

In an attempt to find a good fit for the X-ray diffraction intensities, Drits et al. (1993b) proposed that ferrihydrite consists of a mixture of structures in a disordered array. One of their structural models, the "defect-free ferrihydrite," gives somewhat better agreement with the observed intensities of Figs. 4a and 4b. Their structure has a z-parameter for the Fe sites (with an average occupancy of 0.5) of 0.15, compared with $z = 0.125$, which would correspond to placing the iron atoms at the centers of the oxygen octahedra in the ABAC stacking of close-packed oxygen layers.

We have found that an improved agreement with the observed relative intensities is obtained with a z-parameter of 0.13, the value used for the simulated pattern of Fig. 4c. This gives a separation of iron atom positions in adjacent face-sharing octahedra of 0.226 nm, which is shorter than might be anticipated (see Drits et al., 1993a), suggesting that only one of the two adjacent sites may be occupied, giving the 50% random occupancy of the occupied half of the Fe octahedral sites, as suggested by Drits et al. (1993b). The accuracy with which the relative intensities of the nanodiffraction patterns can be

TABLE I

Estimated Percentages of the Various Structures Identified in Ferritin Cores and in Two Samples of Six-Line Ferrihydrite (Janney et al., 2000c)

	Ferritin cores	75C-6LFh	RT-6LFh
Double-hexagonal (ABACA)	50–70	50–70	50–70
Double-hexagonal with superlattice	—	5–10	—
Hematite	10–20	—	5–10
Maghemite-like	5–10	10–20	10–20
Highly disordered stacking	10	10	10
Double-chain structure	—	5–10	5–10

measured is not sufficient to allow detection of the relatively small effects to be expected from small displacements or differences in occupancies of the oxygen atom sites.

Hematite

Clear evidence has been found that up to one-fifth of the ferritin cores have a structure similar to that of hematite, α-Fe_2O_3. Figure 5a shows the highly characteristic nanodiffraction pattern with an almost square arrangment of spots, which agrees well in symmetry and relative intensities with the simulated pattern of Fig. 5c calculated for the [2,-2,1] orientation of the hematite structure. Similar agreements are found for the [120] pattern (Figs. 5b and 5d) and for other orientations.

The exact composition of the cores giving these patterns cannot be determined. The hematite structure can accommodate some replacement of oxygen by hydroxyl ions, with corresponding vacancies in iron sites (Wolska and Szajda, 1985; Stanjek and Schwertmann, 1992). Any associated variations of unit cell dimensions would be small and not detectable in the nanodiffraction mode.

Magnetite

A small percentage of the ferritin core patterns give evidence for the cubic structure with $a = 0.84$ nm, corresponding to magnetite (Fe_3O_4) or maghemite (γ-Fe_2O_3). A nanodiffraction pattern in the [100] orientation is reproduced in Fig. 6a and compared with the simulated pattern of Fig. 6b. This phase is present in 6LFh and is even more prominent in 2LFh samples. For the clearer patterns obtained from these ferrihydrite samples, the calculated spot intensities give the best agreement with the observations for iron-site occupancies corresponding to the maghemite composition (Janney *et al.,* in press).

Highly Disordered Structures

About 1/10 of the ferritin cores show patterns that indicate a high degree of disorder in the stacking of the close-packed oxygen layers and in the arrangement of the iron atoms. The patterns, such as those of Figs. 7a and 7b, show diffuse streaks and elongated spots in arrays that are reminiscent of such features observed for highly disordered close-packed metal structures (Cowley, 1995).

For the face-centered-cubic close-packing structure, the effects of stacking faults are readily seen in patterns from the [110] orientation Faults in the stacking sequence of the close-packed hexagonal planes of atoms give rise to diffuse streaks in the [111]-type directions, for example, between the

(111)-type and the (200)-type spot positions. Faults on (100)-type planes, such as are common in the 2LFh samples (Janney *et al.,* 2000b), give diffuse streaks in the [100] directions, for example, between the (1,1,-1) and (111) spot positions.

Figures 7a and 7b come from a sequence of patterns recorded with the TV–VCR system as the incident electron beam was scanned slowly along a line through the center of a single ferritin core. They indicate the types of changes of elongated spots and streaks that can occur for patterns taken from points in the core about 1 nm apart. The similarity in the directions of the streaks in the two patterns suggests that the orientation of the close-packed oxygen planes remains the same. However, for the highly disordered structure, the local order within the region illuminated by the incident beam, 0.7 nm in diameter, can change rapidly with the position of the beam. For the dark-field STEM images of such cores, which we obtained using a detector sensitive to changes in diffraction spot intensities, it is to be expected that there will be strong contrast changes within the core images.

General

For the ferritin cores, there is no indication of the double-chain structure found in the 6LFh samples and prominent in the 2LFh samples or of the superlattice of the double-hexagonal structure. However, the highly disordered structure found for ferritin occurs also in 6LFh and is even more common in 2LFh.

For the ferritin cores, as for the ferrihydrite samples, a proportion of the nanodiffraction patterns recorded are such that no definite assignment to a known phase can be made. Such patterns come mostly from crystallites that do not have an orientation close to that for any major zone axis so that the diffraction spots are widely spaced with no apparent regularity. We cannot rule out the possibility that some of these patterns may arise from further minor phases present in very small concentrations and not listed in Table I.

DISCUSSION

Ferritin cores resemble six-line ferrihydrite in that the major phase in both materials has the double-hexagonal structure, which is similar to structures previously proposed for ferrihydrite but is now refined. In both materials the major phase is accompanied by several minor ones, but these minor phases differ in their relative proportions. As seen in Table I, the cores in our horse-spleen ferritin sample come closer to the 6LFh sample formed at room temperature than to the samples of 6LFh formed at

75°C, for which the preparation methods are similar to those for the samples used for earlier structural studies of ferrihydrite (Schwertmann and Cornell, 1991).

Evidence for the polyphasic nature of ferrihydrite has recently been found from selected-area electron diffraction patterns as well as from nanodiffraction studies (Janney *et al.,* 2000c). In earlier nanodiffraction studies of ferritin by Isaacson and Ohtsuki (1980) it was difficult to interpret the patterns because the relatively large convergence angle of the incident beam gave large, and often overlapping, diffraction spots. However, a review of the diffraction patterns published by these authors suggests that some of their patterns could have come from the magnetite-like or hematite-like minor phases rather than from the double-hexagonal structure.

In any structural study made by high-resolution electron microscopy or by electron diffraction it is necessary to consider the possibility that irradiation by the incident high-voltage electron beam can modify the structure of the sample (Hobbs, 1979). Under electron irradiation, transitions from crystalline to amorphous phases are common for organic and biological specimens and for some inorganic and mineral materials. For nanodiffraction with the very intense focused beam of a STEM instrument the loss of crystallinity of silica and some clay minerals has been observed to take place in a fraction of a second (Cowley, 1999). Transitions from one inorganic crystalline phase to another crystalline phase have been observed in several cases during high-resolution electron microscopy (Eyring, 1988).

It is therefore important to establish that the occurrence of the minor phases in the ferritin cores and ferrihydrite is not a result of electron irradiation. Strong evidence is available to suggest that these materials are not affected by electron irradiation, even for the very intense radiation by a focused STEM probe. No evidence for any structural change has been found in high-resolution electron microscopy or in selected-area electron diffraction patterns, which, for ferrihydrite, show agreement with the X-ray powder diffraction patterns (Janney *et al.,* 2000a). The only case of change in the nanodiffraction pattern from a ferritin core is that, on occasion, the pattern shows evidence of a change in the orientation, but not in the structure, of a core crystallite. Such a change may be attributed to the degradation and mass loss of the protein shell that is to be expected under electron irradiation.

Isaacson and Ohtsuki (1980) found no sign of any radiation damage effect for ferritin cores, even though their focused beam was probably more intense than ours because they used a larger angle of beam convergence. In addition, their method of re-

cording the diffraction patterns, using the Grigson method of scanning the diffraction pattern over a small detector, involved a much longer exposure time than our method of using a two-dimensional detector system.

The rapid changes in nanodiffraction patterns recorded at TV rates and occurring in the first fraction of a second of exposure to the intense focused beam for some materials were not observed for ferritin cores. It seems highly improbable that there was an even more rapid initial radiation damage effect, followed by no subsequent damage.

Indications of the chemistry of the ferritin cores available from Mossbauer, EXAFS, and other spectroscopic studies of ferritins necessarily refer to averages over all phases present. Our nanodiffraction data of the individual ferritin cores are insufficient for compositional analysis, and correlation with microanalysis of individual cores has not yet been attempted. It is not possible to determine the extent to which oxygen sites in the structures of the magnetite-like phase and the hematite-like phase are occupied by hydroxyl ions. It is known that some such substitution is possible for the hematite-like phase.

In no case have we observed the appearance of more than one diffraction pattern from any one ferritin core except in the case of the highly disordered structures for which, as may be expected, the pattern of diffuse streaks and diffuse spots changes as the incident electron beam is translated across the core image. This observation is the same for cores of irregular shape or of varying contast in dark-field images as for cores giving regular-shaped, uniform-contrast images. We conclude that a ferritin core normally contains just one crystal in one orientation. The possibility of the presence of smaller regions of purely amorphous material together with the crystal in the core cannot be excluded because the scattering from such material would be much the same as from the radiation-damaged protein shell.

The variations of the contrast within dark-field high-resolution electron microscopy images (Mass-over, 1993) and in our dark-field STEM images of ferritin cores presumably arise in some cases from the occurrence of the highly disordered structures and, in other cases, from variations of thickness rather than variations of structure of the core particles.

These observations suggest that the ferritin cores are normally nucleated at just one point within the protein shell. However, if, as has been proposed, the core is nucleated at several points, the crystallites so formed align themselves to a common crystallographic orientation when they coalesce or one crys-

tallite grows at the expense of the others until only it remains.

Our conclusion that each ferritin core contains only one of the possible crystal structures suggests that the nature of the phase must be determined by the chemical environment in which the core is formed rather than by the specific form or function of the active sites within the protein molecules. This conclusion appears to be consistent with, for example, the observation that magnetoferritin, containing single crystals of the ferrimagnetic iron oxide, magnetite, may be formed when apoferritin protein shells are treated in an appropriate Fe(II) solution and then oxidized (Meldrum *et al.,* 1992).

We suggest that the polyphasic nature of ferritin samples may require some revisions of the interpretations of their physical properties. A major contribution to a measurement of magnetic or other properties may come from a minor component of the sample. A further suggestion is that the differing magnetic or other properties of the minor phases may provide a basis for their separation, which would allow their properties and structure to be studied in more detail.

REFERENCES

Chasteen, N. D., and Harrison, P. M. (1999) Mineralization in ferritin: An efficient means of iron storage, *J. Struct. Biol.* **126,** 182–194.

Cowley, J. M. (1995) Diffraction Physics, 3rd revised ed., Chap. 7 and 18, Elsevier, Amsterdam.

Cowley, J. M. (1999) Electron nanodiffraction, *Microsc. Res. Tech.* **46,** 1–23.

Cowley, J. M., Hansen, M. S., and Wang, S. Y. (1995). Imaging modes with an annular detector in STEM, *Ultramicroscopy* **58,** 18–24.

Crewe, A. V., and Wall, J. S. (1970) A scanning microscope with 5Å resolution, *J. Mol. Biol.* **48,** 375–393.

Drits, V. A., Sakharov, B. A., and Manceau, A. (1993a) Structure of feroxyhite by simulation of X-ray diffraction curves, *Clay Miner.* **28,** 209–222.

Drits, V. A., Sakharov, B. A., Salyn, A. L., and Manceau, A. (1993b) Structural model for ferrihydrite, *Clay Miner.* **28,** 185–207.

Eggleton, R. A., and Fitzpatrick, R. W. (1988) New data and a revised structural model for ferrihydrite, *Clays Clay Miner.* **36,** 111–124.

Eyring, L. (1988) Solid state chemistry, *in* Buseck, P. R., Cowley, J. M., and Eyring, L. (Eds.), High Resolution Transmission Electron Microscopy, pp. 378–476, Oxford Univ. Press, New York.

Harrison, P. M., Fischbach, F. A., Hoy, T. G., and Haggis, G. H. (1967) Ferric oxyhydroxide core of ferritin, *Nature,* **216,** 1188–1190.

Hobbs, L. W. (1979) Radiation effects in analysis of inorganic specimens by TEM, *in* Hren, J. J., Goldstein, J. L., and Joy, D. C. (Eds.), Introduction to Analytical Electron Microscopy, pp. 437–480, Plenum, New York.

Isaacson, M., and Ohtsuki, M. (1980) Scanning transmission electron microscopy of small inhomogeneous particles: Applications to ferritin, Scanning Electron Microscopy/1980/1, pp. 73–80, SEM Inc., AMF, O'Hare, Chicago.

Jambor, J. L., and Dutrizac, J. E. (1998) Occurrence and constitution of natural and synthetic ferrihydrite, a widespread iron oxyhydroxide, *Chem. Rev.* **98,** 2549–2585.

Janney, D. E., Cowley, J. M., and Buseck, P. R. (2000a) Transmission electron microscopy of synthetic 2- and 6-line ferrihydrite, *Clays Clay Miner.* **48,** 111–119.

Janney, D. E., Cowley, J. M., and Buseck, P. R. (2000b) Structure of synthetic 2-line ferrihydrite by electron nanodiffraction. *Am. Mineral.,* in press.

Janney, D. E., Cowley, J. M., and Buseck, P. R. (2000c) Structure of synthetic G-line ferrihydrite by electron nanodiffraction, *Am. Mineral.,* in press.

Massover, W. H. (1993) Ultrastructure of ferritin and apoferritin: A review, *Micron* **24,** 389–437.

Massover, W. H., and Cowley, J. M. (1973) The ultrastructure of ferritin macromolecules. II. The lattice structure of the core crystallites, *Proc. Natl. Acad. Sci. USA* **70,** 3847–3851.

Meldrum, F. C., Heywood, B. R., and Mann, S. (1992) Magnetoferritin: In vitro synthesis of a novel magnetic protein, *Science* **257,** 522–523.

Schwertmann, U., and Cornell, R. M. (1991) Iron Oxides in the Laboratory, VCH, Weinheim, Germany.

Schwertmann, U., Friedl, J., and Stanjek, H. (1999) From Fe(III) ions to ferrihydrite and then to hematite, *J. Colloid Interface Sci.* **209,** 215–223.

Stanjek, H., and Schwertmann, U. (1992) The influence of aluminum on iron oxides. Part XVI. Hydroxyl and aluminum substitution in synthetic hematites, *Clays Clay Miner.* **40,** 347–352.

St. Pierre, T. G., Webb, J., and Mann, S. (1989) Ferritin and hemosiderin: Structural and magnetic studies of the iron core, in Mann, S., Webb, J., and Williams, R. J. P. (Eds.), Biomineralization: Chemical and Biochemical Perspectives, pp. 295–344, VCH, Weinheim, Germany.

Towe, K. M., and Bradley, W. F. (1967) Mineralogical constitution of colloidal "hydrous ferric oxides," *J. Colloid Interface Sci.* **24,** 384–392.

Wolska, E., and Szajda, W. (1985) Structural and spectroscopic characteristics of synthetic hydrohaematite, *J. Mater. Sci.* **20,** 4407–4412.